JOURNAL OF SPACECRAFT AND ROCKETS
Vol. 44, No. 1, January–February 2007

Finite Element Modeling and Analysis of Large Pretensioned Space Structures

Thomas C. Jones* and Hilary Bart-Smith†
University of Virginia, Charlottesville, Virginia 22903
Martin Mikulas‡
National Institute of Aerospace, Hampton, Virginia 23666
and
Judith Watson§
NASA Langley Research Center, Hampton, Virginia 23666

DOI: 10.2514/1.23116

Pretensioned structures have great potential for providing the required size, stiffness, and packaging efficiency for large deployable space structures such as radio antenna, radar, and solar reflectors. These structures, however, are difficult to model correctly using standard numerical techniques, such as finite element analysis, and the current lack of literature on a robust modeling methodology can lead to analysis errors and wasted time. This paper details the static and dynamic behavior of pretensioned systems in their analytical forms and demonstrates how that behavior can be characterized using commercially available finite element software. This study was performed using ABAQUS Standard/CAE, but the methodology could be applied to any of the major finite element packages. A simple cable–beam system and a pretensioned truss structure are analyzed to verify the methodology and illustrate its suitability to modeling the behavior of complex pretensioned structures. This paper provides an introduction and overview to modeling and analyzing pretensioned space structures for analysts and engineers familiar with modern finite element methods.

Nomenclature

A_c = cable cross-sectional area
A_s = stay cross-sectional area
E_c = cable elastic modulus
E_s = stay elastic modulus
F_b = equilibrated beam load
F_+ = induced tension
F_- = induced compression
f_{n1} = fundamental natural frequency, Hz
h = stay connection height
I = moment of inertia
K = equivalent spring stiffness
K_c = radius of gyration
K_s = stay lateral stiffness
L = column length
L_s = stay length
P = applied load
P_{cr} = Euler buckling load
r = radius of circular tube
T_f = final equilibrated tension
T_i = initial pretension
α = height-to-length ratio or coefficient of thermal expansion
Δ = change in vertical displacement
δ = change in cable–beam length
δ_o = initial geometric eccentricity
θ = slope or angle
ρ_b = beam density
ρ_c = cable density
ω_{n1} = fundamental circular frequency, rad/s

Received 10 February 2006; revision received 7 July 2006; accepted for publication 8 August 2006.

*Ph.D. Candidate and Research Assistant, Department of Mechanical and Aerospace Engineering. Student Member AIAA.
†Assistant Professor, Department of Mechanical and Aerospace Engineering. Member AIAA.
‡Research Engineer. Fellow AIAA.
§Research Engineer, Structural Mechanics & Concepts Branch. Senior Member AIAA.

I. Introduction

AT NASA and throughout the space industry there is currently great interest in building very large structurally efficient space structures to function as radar antennas, parabolic reflectors, solar arrays, and radio interferometers. Pretensioned structures have great potential for providing the required size, stiffness, and volumetric packaging efficiency for these applications. These structures employ tensioned members to stabilize and significantly augment the lateral stiffness of the primary compressed members without the addition of significant mass or volume. Pretensioned structures, however, can be complicated and problematic to model using current FEM packages and present unique challenges to the analyst. The static and dynamic behavior of these structures is governed principally by the relative stiffness and mass of the members and by the level of applied tension. However, nonlinear lateral and material stiffness and pretension-induced geometric eccentricities also influence this behavior and must be considered.

Literature on the modeling and analysis of large pretensioned space structures using commercial FEM is scarce. Available research typically falls into one of two categories: 1) exact numerical or design formula descriptions of specific behaviors or structures or 2) results of experimental work on particular prototypes with some comparison to finite element analysis. Pretensioned structures are typically statically indeterminate and behave nonlinearly; they therefore are not easily described analytically. As a result, exact formulations that have been presented use only simple geometries [1–7]. Engineering design formulas, although employed in more complex structures, remain applicable only within strict geometric and loading constraints [8,9]. As a consequence, FEM must generally be used for the analysis of current pretensioned structures. Although a large body of experimental work has been published on this class of

structure, it gives little practical information to analysts faced with the modeling issues that these structures introduce and provides only cursory explanations of the methodology used [10–19]. Documentation included with commercial FEM packages also typically has few relevant examples and does not discuss cable/stay modeling or applying pretension to member sets [20].

Accurate and efficient modeling and analysis of large pretensioned space structures requires a familiarity not only with the characteristics of these structures, but with the capabilities and application of modern FEM. Because of the size of these structures, full-scale ground testing is often not feasible and emphasizes the requirement for precise FEM models. This paper focuses on the application of *commercial* FEM packages due to their pervasive use in industry and government and due to the interest these groups have in using their existing software to analyze this class of structure. Current FEM allows model data to be easily exchanged and updated and provides an ever expanding set of advanced modeling and analysis tools to the analyst, as compared with specialized FEM codes with limited scope and applicability. ABAQUS Standard/CAE was employed in this study for its nonlinear and pretension modeling capabilities and for its advanced material definition tools. However, the methodology described could be implemented in any advanced nonlinear FEM package. ABAQUS CAE incorporates both a pre- and postprocessor that allows all modeling and analysis to be completed using only one application. This is coupled with a built-in scripting capability that allows rapid model development and analysis using a single piece of code. Wire-frame elements, including truss/rod and beam/bar elements, are used and recommended due to their geometric and meshing simplicity and computational efficiency. As the majority of large pretensioned structures consist of long slender members and cables, wire elements are ideal for modeling the entire structure and provide accurate results for these geometries without having to construct and mesh a detailed three-dimensional solid model.

This paper provides an introduction and overview to modeling and analyzing pretensioned space structures for analysts and engineers familiar with commercial FEM codes. The key areas of concern for modeling these types of structures are discussed, including member and joint definition, cable modeling, and pretension application. Frequency and static load analyses are performed on two structural models: a simple cable–beam system and a pretensioned truss. These examples illustrate the application of the methodology and demonstrate its suitability for modeling increasingly complex pretensioned structures.

II. Analytical Characterization of Pretensioned Structures

Large flexible pretensioned structures are challenging to describe via closed-form solutions without significant linearization due to their nonlinear mechanics, lateral stiffness properties, and large number of members. This section discusses analytical solutions for certain behaviors that are encountered in pretensioned structures, specifically, frequency and buckling behavior, nonlinear lateral stiffness, and eccentric deformation and loading of the members. Furthermore, these solutions are explored to develop general conclusions about the response of pretensioned structures and general principles to guide the modeling of such structures.

A. Natural Frequencies of Axially Loaded Beams and Cables

The analytical equations that describe the frequencies of the members in tension and compression are examined to elucidate the global behavior of pretensioned structures. Using summation of forces and moments on a single beam element, it is possible to find an expression for the fundamental circular frequency of a pinned–pinned beam [21]:

$$\omega_{n1} = (2\pi) f_{n1} = \pi^2 \sqrt{\frac{EI}{\rho A L^4}\left[1 \pm \frac{T}{P_{\text{cr}}}\right]} \tag{1}$$

In Eq. (1), the $\pm T$ corresponds to a tensile or compressive load, respectively. Typically for pretensioned systems, a set of beam members are compressed by a set of tensioned cable members. An expression for the fundamental natural frequency of a pinned–pinned cable can be derived by expanding Eq. (1),

$$f_{n1} = \frac{\pi}{2}\sqrt{\frac{EI}{\rho A L^4} \pm \frac{EI}{\rho A L^4} T\left(\frac{L^2}{\pi^2 EI}\right)} = \sqrt{\frac{\pi^2 EI}{4\rho A L^4} \pm \frac{T}{4\rho A L^2}}$$

and removing the term that corresponds to the bending stiffness, leaving

$$f_{n1} = \frac{1}{2}\sqrt{\frac{T}{\rho A L^2}} = \frac{1}{2}\sqrt{\frac{T}{mL}} \tag{2}$$

Equations (1) and (2) predict that, as the compressive force in the beam approaches the Euler buckling load, *or* if the tension in the cable approaches zero, the frequency will approach zero. This creates a coupling between the properties and loading conditions of a cable–beam system, which is explored in Sec. IV. This is a property of all pretensioned systems, although the critical loading point becomes harder to determine as additional members are added. Local cable modes also tend to fragment the frequency vs pretension load plot by interacting with the global modes. The condition of zero tensile load in the cables correlates to the point of slackening and is an extremely important consideration in static and dynamic analyses. This is detailed and illustrated in the truss example of Sec. V.

B. Material, Geometric, and Nonlinear Lateral Stiffness

Pretensioned structures derive their structural and packaging efficiency from using primarily slender members in tension with a few stout compression members. They achieve a high degree of stiffness from the geometry, location, and properties of the stays that stabilize the structure. Material stiffness is the inherent stiffness of a structure due to the mechanical properties of its members. Structures that depend primarily on material stiffness to sustain loading, however, pay a penalty in mass and volume to do so. Pretensioned structures rely heavily on the geometric stiffness provided by the tension in the members and the lateral stiffness provided by the increased depth of the structure. The addition of cables or stays is equivalent to attaching elastic restraints to the structure, to resist vertical motion. The structure's deformation in certain modes is thus restrained due to the locations of the cable connection points [1].

The lateral stiffness provided to a member via a stay depends nonlinearly on the angle at which it is connected. To illustrate this concept, we examine the pretension stayed column in Fig. 1. A rigid column is attached to a wall via a pin joint and is provided lateral stiffness in the vertical axis by two tensioned stays. A vertical load is applied at the end of the column, producing additional tension in the upper stay, a compressive load in the lower stay, and a displacement at the tip.

If the compression from P is less than the initial pretension in the lower stay, then the lateral stiffness can be found in terms of the stay properties (n.b., the tension does not factor into the stiffness equation):

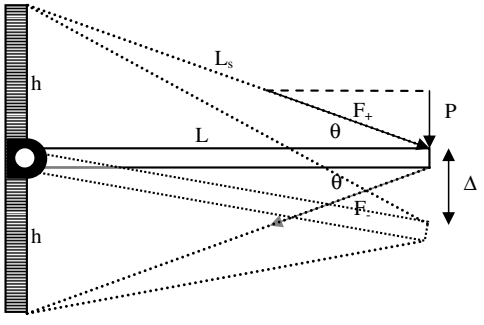

Fig. 1 A stayed column with an applied vertical load.

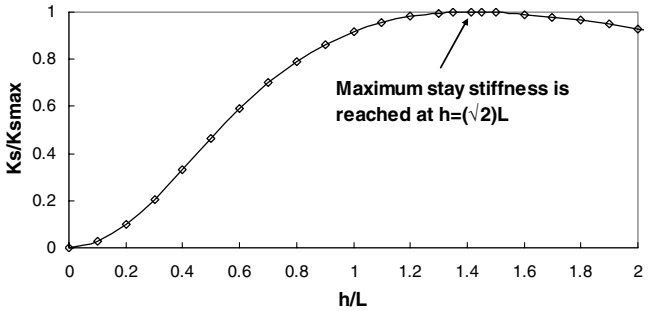

Fig. 2 Normalized lateral stay stiffness vs the ratio of height to column length.

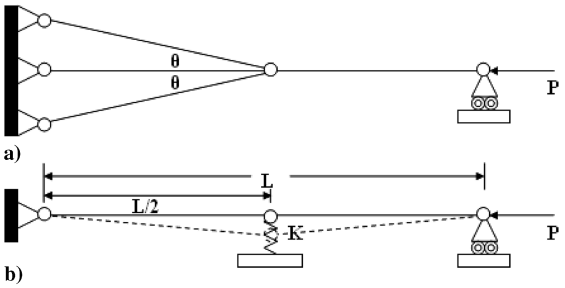

Fig. 3 A stayed column represented by an equivalent beam with spring support.

$$P = 2[K_s]\Delta = 2\left[\frac{E_s A_s}{L_s}\sin^2(\theta)\right]\Delta \tag{3}$$

Equation (3) illustrates that the lateral stiffness provided by a tensioned member has a second-order nonlinear dependence on θ. This nonlinearity must be taken into consideration when designing these structures, specifically when sizing the stays, and the central support column. If the lateral stiffness provided by one stay is rewritten in terms of the column length and constant α, we have

$$K_s = \frac{E_s A_s \alpha^2}{L(\alpha^2+1)^{3/2}} \tag{4}$$

Equation (4) is used to plot $K_s/K_{s\ \max}$ vs α (Fig. 2), demonstrating that a maximum stiffness is attained at $\alpha = \sqrt{2}$, or $\theta = 54.74$ deg, and the function is not simply quadratic as it appears in Eq. (3). $\theta = 54.74$ deg often appears as an optimum in structural applications and in this case marks the transition point between the increasing contribution of the vertical component of stay stiffness (as θ increases, K_s increases) and the detrimental effect of increasing the stay length (as L_s increases, K_s decreases).

C. Buckling in Pretensioned Space Structures

Buckling can be initiated in pretensioned structures from a number of sources including stresses from the initial tensioning, compressive forces during equilibration, and various external loads. The critical buckling loads for individual members of a pretensioned structure are found by taking into account these loads and the existing connection boundary conditions. As a simple example, the beam buckling load for a single inline cable–beam system after equilibration is found to be the Euler buckling load minus the induced compressive force from pretensioning minus any external axial forces: $P_{\text{cr}} = P_{\text{Euler}} - F_b - F_{\text{ext-axial}}$.

For members that are stayed along their length, or structural mechanisms that are restrained by tension members, the lateral stiffness is included analytically as an added elastic restraint at the point(s) of contact. The added stiffness of a stay is normally designed and placed to suppress a specific buckling mode. A detailed study on the optimization of such structures was done by Mauch and Felton [1]. If we take the case of the stayed column again but assume that the column is now pinned at both ends and loaded axially, the fundamental buckling mode will be in the shape of a half-sine wave. To suppress this mode, stays must be attached at the midpoint of the column and sized so that they force the column to buckle into its second mode (Fig. 3a). To find the required stiffness of the stays, an equivalent beam is used with an elastic support in the lateral direction that suppresses the desired mode (Fig. 3b).

It can be shown that the buckling load of a pinned–pinned beam or a column with an elastic support at $L/2$ (Fig. 3b) is a function of the stiffness of that support [22]:

$$P_{\text{cr}} = \frac{KL}{4} \tag{5}$$

Therefore, we can set Eq. (5) equal to the desired second mode solution of a standard pinned–pinned beam and find the required stiffness of the support:

$$\frac{KL}{4} = \frac{4\pi^2 EI}{L^2} \tag{6a}$$

or

$$K = \frac{16\pi^2 EI}{L^3} \tag{6b}$$

For values of P_{cr} that are less than the second mode solution but greater than the first mode, the beam will buckle into the first mode shape but at a higher value of P. For the two-stay supported column of Fig. 3a, we can use Eq. (3) to find the required axial stiffness of the stays:

$$K = 2K_s = \frac{2E_s A_s}{L_s}\sin^2(\theta) \tag{7}$$

Setting Eq. (7) equal to Eq. (6b), converting the stay length to column length, and solving for $E_s A_s$, we have

$$E_s A_s = \frac{4\pi^2 E_c I_c}{\sin^2(\theta)\cos(\theta) L^2} \tag{8}$$

Therefore, by adjusting the modulus or area of the stays at a given angle, the desired lateral stiffness can be achieved to suppress the first mode. Additional stays may be added in a similar manner to restrain higher modes.

D. Geometric and Load Eccentricities

The slender and flexible members of these structures are particularly susceptible to geometric and loading eccentricities, which impact their effective stiffness properties. For the pinned–pinned beam, the change in effective axial stiffness from an initial geometric eccentricity is related to the magnitude of the initial deflection and the radius of gyration by Eq. (9):

$$\frac{EA_{\text{eff}}}{EA} = \frac{1}{1+(1/2)(\delta_o/K_c)^2}, \quad \text{where } K_c = \sqrt{\frac{I}{A}} \tag{9}$$

If the beam is a circular shaft, as is often the case for compressive members of pretensioned structures, Eq. (9) can be rewritten in terms of the shaft's radius [8]:

$$\frac{EA_{\text{eff}}}{EA} = \frac{1}{1+(\delta_o/r)^2} \tag{10}$$

Typically, $r \ll L$; thus, from Eq. (10), it can be observed that, if the deformation is on the same order as the radius, the stiffness will be halved. For a slender member the L/D ratio may approach 100; thus, a 0.5% deformation will cause a 50% degradation in axial stiffness.

The reduction in effective axial stiffness is due to the increasing participation of the bending stiffness in resisting the load. As δ_o grows, the bending moment increases rapidly, and the load required to reach a specific lateral deformation decreases at the same rate. Even though the critical buckling load remains the same for any δ_o, it

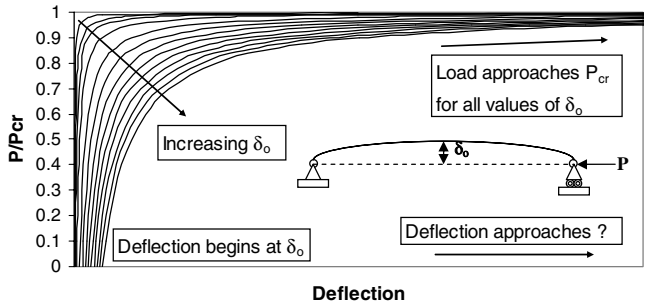

Fig. 4 Effect of initial deformation on P_{cr}.

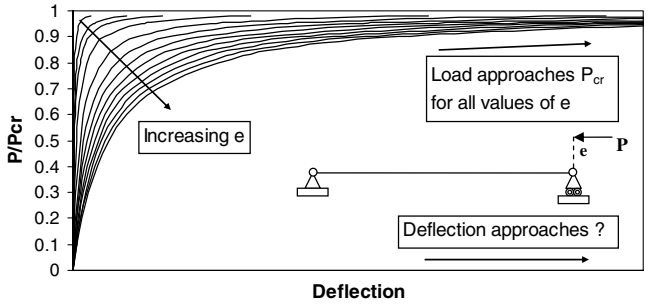

Fig. 5 Effect of load eccentricity on P_{cr}.

is reached theoretically only at infinite deformation (Fig. 4). In reality, the member will fail at some peak deformation due to material breakdown; thus, the initial deformation dictates at what load that failure will occur. This is important to understand as, often in modeling, failure stresses are not included in the material definition for simplicity, and the FEM program will not alert the analyst to a critical stress state unless it has been explicitly defined. Eccentric loading affects the axial stiffness in a very similar manner (Fig. 5), but the failure load is determined by the magnitude of the load offset, *e*.

The buckling behavior is complicated by the fact that the deformation of eccentrically loaded or deformed members is often limited via directly applied elastic restraints (in the form of tension cables, for example) or the rigidity of the surrounding structure. Therefore, before the bending limit is reached those high stresses can be redistributed and cause bending and compression of other members. In Sec. V, it is demonstrated that, due to the effects of these eccentricities on pretensioned space structures, traditional buckling analyses cannot be performed in FEM when considering local member buckling.

III. Modeling Methodology for Pretensioned Structures Using Finite Element Methods

A. Member and Joint, Definition, and Assembly

Defining the geometry of the structure and accurately modeling the interactions and constraints between members is of fundamental importance. When using wire-frame elements, geometry construction can be performed rapidly by defining datum points at the key nodes of the structure (member connection points) and connecting those points to create the base structural members (Fig. 6).

This method allows swift and simple adjustment of the structural dimensions and lends itself well to scripting, permitting automated geometry creation and meshing to be included as part of the analysis process. The datum-point method also does not require the redefinition of any included connectors or constraints, as the actual reference points are adjusted, as opposed to a sketch plane containing those points. If a single part consists of multiple members, such as the truss shown in Fig. 6, those members are considered *fixed* together in FEM. Cable members are therefore added as individual parts and

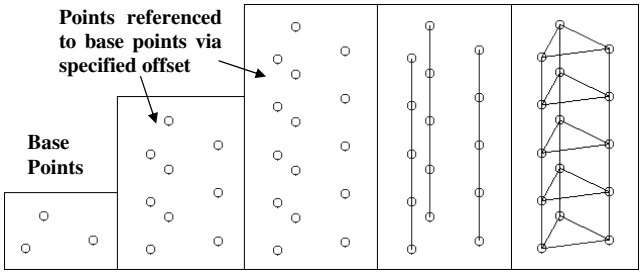

Fig. 6 Datum-point geometry construction.

attached to the base structure of compressed members via connectors.

The joints of these structures must also be carefully modeled, especially if the connecting members do not all meet at a single point. Modeling solid joints using only wire-frame elements is accomplished by using both multipoint constraints (MPCs) and connectors. MPCs are used to simulate properties such as coupling or rigid body connections between regions of a model. They differ from connectors by having a well-defined master–slave relationship and requiring the use of only independent nodes. They also do not offer behavior options such as damping or elasticity. A joint can usually be considered rigid in comparison to the other members of a large pretensioned space structure; thus, any elements of the wire-frame model that fall within the dimensions of the joint must be rigidly fixed to a reference point at which the major structural members meet. For the truss of Fig. 6, this is achieved by coupling all the nodes at and between the batten-joint interfaces to the reference point and kinematically constraining all 6 degrees of freedom of those points to the movement of the joint (Fig. 7).

In a solid three-dimensional model, the diagonals (cable members) would be connected directly to the joint. In this case, for efficiency, each diagonal is connected to the imaginary point where its load path crosses the batten axis as shown in Fig. 7. JOIN connectors model the pin joints, enforcing free rotation about the x, y, and z axes and keeping all displacements the same at the connection point between members. When multiple nodes are located at the same coordinates, it is extremely important to make sure the correct nodes are selected for the connector definition, as a mistake may result in analysis errors from incompatible displacements. It is also a good custom in modeling these structures to identify the compressed base members as the master nodes and elements and to connect the tension members to them.

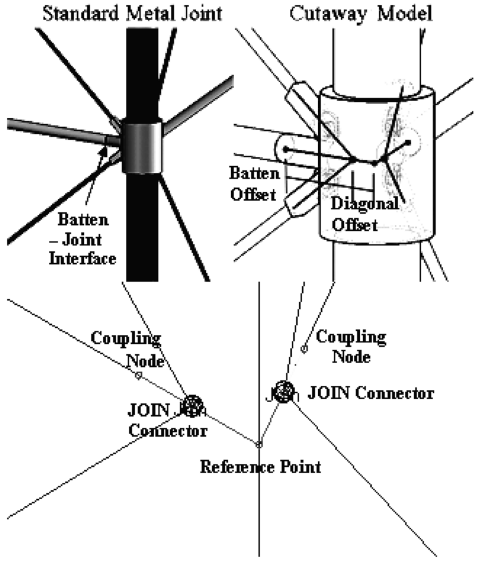

Fig. 7 Joint model using MPCs and JOIN pin-joint connectors.

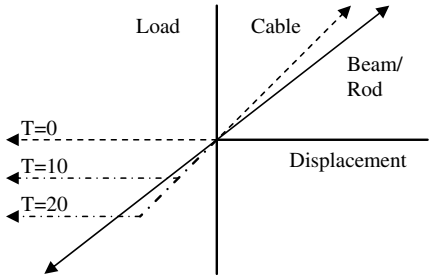

Fig. 8 Typical cable and beam/rod load-displacement plots.

B. Modeling Cable Elements

A key issue in modeling pretensioned structures is the exclusion of cable elements from current FEM packages (e.g., ABAQUS, NASTRAN, and ANSYS). A cable behaves like a rod under a tensile load but loses stiffness once it reaches a state of compression (Fig. 8). If the cable is pretensioned, it can sustain compression up to its initial load before losing stiffness. Conversely, the stiffness of beams and rods is identical in both tension and compression.

The most appropriate elements for modeling tensioned cables in a static FEM analysis are truss elements ("rod" or "spar" elements in NASTRAN and ANSYS) that allow only axial forces and rigid body displacements (no moments or forces perpendicular to the centerline are supported). However, truss elements have stiffness in compression; thus, a method must be found to negate the member stiffness once a compressive state has been reached.

In ABAQUS, the member stiffness can be negated under compressive loads via the use of an option called "no compression." When added after the elasticity definition in the material description, members employing that material will have zero stiffness in compression. The discontinuous nature of the load-displacement curve can cause computational and stability issues when modeling the cables with multiple elements due to the problem of calculating internal nodal displacements when the stiffness matrix is nullified. Truss elements also impose constraints on the rotational degrees of freedom and can be difficult to include in complex structures with other less constrained elements, such as beams. However, when a single truss element is connected using pin joints (JOIN) so that it can rotate with the structure and the no compression option is employed, it provides one of the best representations of a cable available in FEM for performing static analyses. *Note that although a single beam element could perform the same function, it would require additional constraints and would only increase the computational cost of the analysis.*

Dynamic analyses must include the lateral inertia of the cable; therefore, the use of a single truss element is not sufficient. In this case, multiple beam elements are used to represent the cable, and it is assumed that the cables remain in tension throughout the analysis. The fundamental frequency of an axially loaded simply supported beam was given in Eq. (1). The general form of this equation for any boundary conditions is presented in Eq. (11) and relates the loaded and unloaded beam frequencies through a term involving the tension and critical buckling load [23]:

$$\omega_n|_{T\neq 0} = \omega_n|_{T=0}\sqrt{1 \pm \frac{T}{P_{\text{cr}}}} \tag{11}$$

The term in square roots reveals the criterion that allows the use of beam elements to model cables for dynamic and frequency analyses. As the cables remain tensioned, the plus sign is used, and although the bending stiffness term cannot be eliminated, the tension term can dominate it. Thus, *if the tension in a cable is much greater than the buckling load of the beam representing it, then beam elements can accurately approximate that cable in tension.* For dynamic analyses, the analyst must check that the $T \gg \mathrm{P_{cr}}$ criterion remains valid over the entire analysis. The number of beam elements used in the cable should correlate to the number of modes required; thus, for higher modes, more elements are needed. Multiple truss elements are not recommended for modeling the tension members of pretensioned structures due to the required load equilibration step in every analysis. The twisting in the structure during equilibration can cause displacement incompatibilities in the internal nodes of a cable modeled with truss elements, often resulting in the breakdown of the analysis.

C. Pretensioning a Set of Structural Members

Pretension is applied to an actual structure via a number of methods. Often the structure will be mechanically deployed and the tension members are stretched to the final loaded condition as the rest of the frame is locked into place. Strain energy devices, such as springs or elastic materials, can also be used to deploy relatively light loads and induce the required pretension in the system. Compression members can be deployed via inflation, which in turn applies load to the tension members, but this is generally performed in combination with a mechanical device to ensure complete inflation and proper load distribution. Finally, thermal strain can be induced in a structure to pretension the members, but again would typically include mechanical assistance due to the small axial stresses afforded by the method and the danger of damaging components under high thermal loads.

Applying the pretension correctly to members of a structure in a FE analysis is one of the most critical steps in these analyses, and several simple models were run to check the validity of the FEM approach against analytical solutions. There are several methods for applying the tension, two of which are useful for unrestrained space structures. The most basic method of tensioning a cable is to apply an axial force at one end equal to the desired pretension. This is simple for a single cable lying in one of the principle directions, but it quickly becomes onerous for multiple tensioned members in different planes. Local coordinate systems would have to be assigned to each member along with individually defined loads. Directly applied loads on unrestrained models also cause computational errors, even if the loads are applied in equal and opposite directions. In the following techniques, thermal or mechanical stress can be applied initially without deformation of the members (although some deformation will occur during equilibration) and without the need for restraining the system after equilibration.

A common method of applying pretension to a model is through the use of a thermal preload coupled with appropriately selected coefficients of thermal expansion (CTEs). By calculating the thermal strain required to induce a specific tension in each set of members, a temperature field can be applied to the whole model that loads all of the selected members to the required pretension. The thermal strain is defined as the CTE multiplied by the change in temperature, ΔT:

$$\varepsilon_{\text{therm}} = \alpha \Delta T \tag{12}$$

Using Hooke's law we can rewrite Eq. (12) in terms of stress and thus in terms of the tension in the member:

$$\Delta T = \frac{\varepsilon}{\alpha} = \frac{\sigma}{\alpha E} = \frac{T}{\alpha E A} \tag{13}$$

Therefore to get an initial tension of T in a particular member(s), the analyst can set ΔT to a constant and adjust α to get the desired pretension or vice versa. The advantage of this method is that the analyst needs to assign only a *single* temperature field to pretension the entire structure, and it can be implemented in most FEM packages. The problem, however, is making sure the CTEs, temperature field, and geometry are such that the members are correctly tensioned, which can be time consuming.

Some advanced commercial FEM codes allow the user to directly input pretension loads without the use of an equivalent thermal load. For example, ABAQUS CAE allows initial prestress to be specified via command line input. These command lines are added after the material property definition in the input file using the keywords editor. Given a set of like cable members called "setname" with tensions $T = 20$ lb and areas $A = 0.01$ in.^{2}, the stress would be

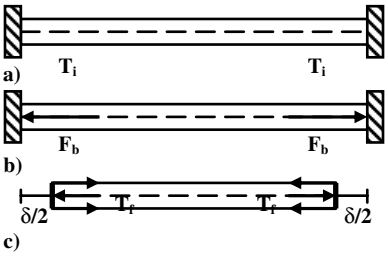

Fig. 9 Pretensioning a beam with a tensioned cable pinned at each end.

$\sigma = T/A = 2000$ lb/in.^{2}, and the following lines would apply this prestress (and thus a pretension of 20 lb) to all the members in that set:

*INITIAL CONDITIONS, TYPE = STRESS
setname, 2000.

The obvious advantage of this technique is its simplicity, but considering that the CTE method requires only a single temperature load once set up, the current method might suggest a longer update time if pretensions are changed. However, this is not true as sets must be created to assign material properties and boundary conditions to the tension members and the same sets can be used to assign prestresses. Multiple member sets can be assigned stresses by repeating the preceding command lines and can be easily updated in either the input file or keywords editor of CAE. It should be noted that the initial stresses are not equilibrated when applied; therefore, for *any* pretensioned structural analysis a static step *must be* run first for the structure to reach a state of equilibrium.

It is important to be aware that, regardless of the method used to apply the prestress, the actual preload in the cable elements will depend on the relative stiffnesses of the cable and surrounding structure. To illustrate this effect, we shall again consider a simple cable–beam system (Fig. 9). A hollow cylindrical beam has a cable attached via pin joints to each end, and the entire system is initially unloaded and fixed at each end (Fig. 9a). An initial tension is applied using either of the methods described (Fig. 9b) while the beam remains fixed. The boundary conditions are then removed and a static step is run to allow the loads to equilibrate, leaving the final pretensioned unrestrained system (Fig. 9c). T_i must be found so that the force in the beam is at the required level after equilibration. Using Hooke's law, one can determine the final equilibrated tension and equilibrated beam load via

$$T_f = \frac{E_c A_c}{L}\delta \tag{14a}$$

and

$$F_b = \frac{E_b A_b}{L}\delta \tag{14b}$$

Both the cable and beam deform by an equal amount in the final state; thus, using Eqs. (14a) and (14b),

$$T_f = \frac{E_c A_c}{E_b A_b} F_b \tag{15}$$

The sum of the forces must be the same before and after equilibration; therefore, using Eq. (15),

$$T_i = F_b + T_f = F_b\left(1 + \frac{E_c A_c}{E_b A_b}\right) \tag{16}$$

This simple pretensioned system demonstrates how the initial tension in a cable member is redistributed after equilibration due to the deformation of both members. Equation (16) illustrates that if the axial stiffness of the tensioning member is much smaller than the compression member, the final force in the beam is approximately equal to the initial tension in the cable (17). If, however, the axial stiffness of both members is of the same magnitude or the tensioning member is stiffer, then the magnitude of the required initial tension can increase significantly and depends on the axial stiffness ratio (18).

$$\text{If } E_c A_c \ll E_b A_b, \quad \text{then } T_i \cong F_b \tag{17}$$

$$\text{If } E_c A_c \gg E_b A_b, \quad \text{then } T_i \cong \frac{E_c A_c}{E_b A_b} F_b \tag{18}$$

These results have several modeling implications for more complex pretensioned systems. To overcome the added stiffness in the system and reach the required load, a structure with stiff tension members will experience larger deformations and higher stresses during pretensioning. The tension cables often apply load to multiple members in nonaxial directions, which makes it challenging to determine a simple analytical expression for the equilibrated loads given the initial tension, as was found in Eq. (16). This is especially true for truss structures that use crossed tension diagonals as support elements. Therefore, when designing and modeling pretensioned space structures, case (17) is often used. Tension members with significantly reduced stiffness act in effect like constant-force springs. This renders the structure statically determinate and allows the approximation of equality between the initial pretension and final load on the compression members. Soft tension members not only simplify design calculations but also allow far less stress to be applied to a real structure during the pretensioning process. It should be noted, however, that soft tension members are usually employed as stabilizing elements and their mass is not significant when compared with other major structural elements. When tensioned members have significant payload mass attached to them, then higher stiffness is often necessary so as not to critically reduce the system frequency of the entire structure and allow for a simpler control system. High-stiffness tension members have different final tension levels to the initially applied preload; thus, an analyst must be careful to iterate the initial tension until the desired resultant level of preload is achieved. This can be automated via a simple script.

IV. Cable–Beam Example: Frequency Analysis

Frequency analyses are run for the cable–beam system shown in Fig. 9c to illustrate the characteristic behavior of a pretensioned structure when the tension, mass ratio, and axial stiffness ratio are varied. The cable–beam system is one of the simplest pretensioned structures possible, but it clearly demonstrates the effect of self-stress on frequency response. The system is unrestrained during the analyses, and the cable-to-beam axial stiffness and density ratios are given the values 1/100, 1, and 100 to provide a broad basis of comparison. The length and total cross-sectional area of the two members are the same in this case so that the density is directly proportional to the mass; however, the moment of inertia of the cable is several orders of magnitude less than the beam. The graphs in Fig. 10 show the results of these analyses and plot the fundamental frequencies of the cable–beam system as the pretension load is adjusted from zero to the beam buckling load.

The mesh density and element types are chosen from an initial study run for the beam and cable members. As large pretensioned space structures consist of numerous slender members under generally small external loads, Euler–Bernoulli elements are perfectly adequate and are computationally less expensive for most analyses than elements based on Timoshenko beam theory. Hybrid elements, used for slender members in flexible structures, help convergence in these models by calculating the axial forces separately from the bending moments, which are often orders of magnitude smaller. For pretensioned structures with large numbers of tension members, it is strongly suggested these elements are used to avoid typical convergence difficulties caused by using standard elements. Hybrid linear beam elements, B31H elements in ABAQUS, are used in these analyses for both the cable and beam. Hybrid versions of both beam and truss elements are available.

The three graphs in Fig. 10 represent the three different cable-to-beam density ratios. In Fig. 10a, the cable is only 1% of the mass of the beam, and it has very little effect on the system, while in tension,

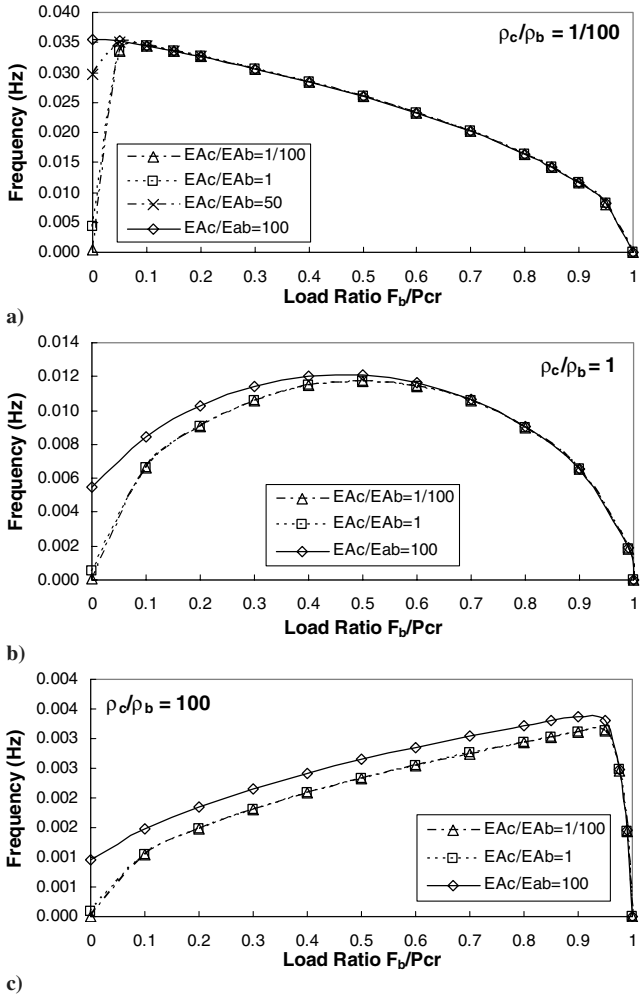

Fig. 10 Frequency vs tension plots for the cable–beam system.

due to its mass contribution. As the preload goes toward zero, however, the system frequency rapidly approaches zero, and the effect on the fundamental mode becomes significant. Because of the use of beam elements, the frequency never reaches zero as the small amount of bending stiffness in the cable always gives a nonzero frequency. This effect is amplified in all cases if the bending stiffness of the cable elements is significant, as for the cases in which the cable-to-beam axial stiffness ratio is 100. As the tension decreases, it no longer dominates the bending term, and as the stiffness ratio increases, the system frequency at zero load will increase. In Fig. 10b the density of the cable and beam are equal. The frequency values thus follow a smooth transition between primarily cable dominance on the left to primarily beam dominance on the right. As both members have the same mass, the system behavior is dictated by the level of pretension and is fully coupled. Figure 10c plots the case in which the cable represents the majority of the mass and the behavior is therefore the opposite of the first case. The frequency values are only influenced by the beam as the pretension approaches the beam buckling load.

The shape of these plots represents the interaction that occurs in any pretensioned structure when adjusting the mass, stiffness, and pretension levels of the tensioned and compressed members. Typically, when the tension members are solely providing support and stability to a structure, the frequency plots look like Fig. 10a, as the tension members represent far less mass than the base compressive members. However, *an analyst looking at a similar plot to those in Fig. 10 could determine the mass influence of the tension members, whether high-stiffness elements were used, and what buckling limit the system had*. Multiple truss elements could be used for the cable in this particular model, due to the lack of twisting, with similar results. The nonzero frequency effect with increasing stiffness would, however, be eliminated, and all the plots would look essentially like the $EA_c/EA_b = 1/100$ cases. It is also noted that if a single truss element, recommended for static analyses, is used for the cable in a low ρ_c/ρ_b frequency analysis, the results show excellent convergence to the previous cases, providing the tension does not approach zero. This again is due to the reduced influence of mass on the system when there is tension in the cable. Last, due to the requirement of an equilibration step before the frequency analysis, a *nonlinear* static step must be used. If a linear analysis is used, the pretensioning will not be included in the frequency analysis.

V. Tensioned Truss Example: Axial, Bending, and Torsion Load Analyses

The second example studies the effects of cable slackening under external load on a four-bay pretensioned truss when the diagonal cables are offset at the joints (Fig. 11). The model is based upon an experimental rigidizable truss, recently developed at NASA Langley Research Center. The vertical members (longerons) are rigidizable composite tubes, and the horizontal members (battens) are aluminum tubes. The soft tension members (one set highlighted) are steel cables with inline springs providing the pretension, and the stiff diagonals are telescoping steel rods laced in opposition to the soft diagonals. The stiff diagonals are tensioned by the soft, resulting in three pairs of equally tensioned cables in each bay. From the analyses, it is noted that the diagonal offsets *do not* affect the load equilibration of the truss.

A. Axial Load and Buckling Analyses

Geometric and load eccentricities (discussed in Sec. II.D) were shown to have a significant effect on the structural behavior of slender pretensioned structures. Therefore, the first series of analyses are designed to quantify the effect that the joint offsets have on the truss under axial loading. The diagonal offset values are adjusted from $0 \sim 5\%$ of the batten length, with pretensions of 10, 20, and 40 lb. A script is used to concurrently adjust the diagonal and batten offsets (to simulate scaling the joint) and create a new model for each case without requiring manual remodeling. As the offsets and preload are increased, the amount of initial deformation in the longerons is amplified, significantly reducing their effective axial stiffness.

Typically the critical axial load is found by performing a linear perturbation buckling analysis in FEM. This type of analysis is based on the assumption that the structure is stiff and stable in its base state. Eccentrically deformed pretensioned structures, however, due to the curvature in their members, cannot be considered initially stiff and will bend locally under axial load. If buckling analyses are run for the

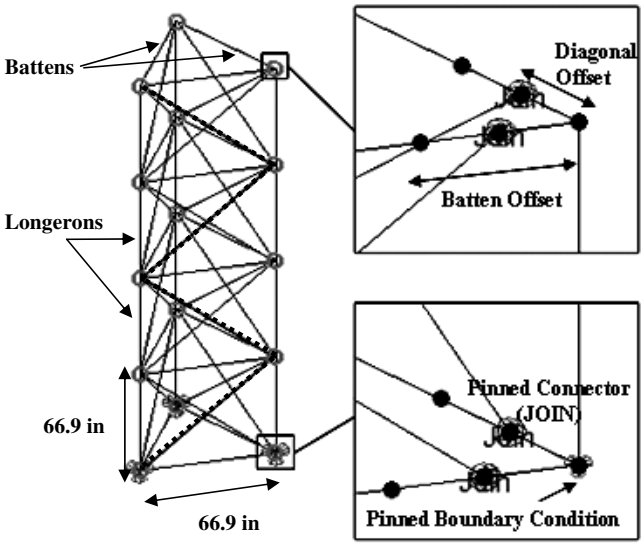

Fig. 11 Tensioned truss with offset diagonals.

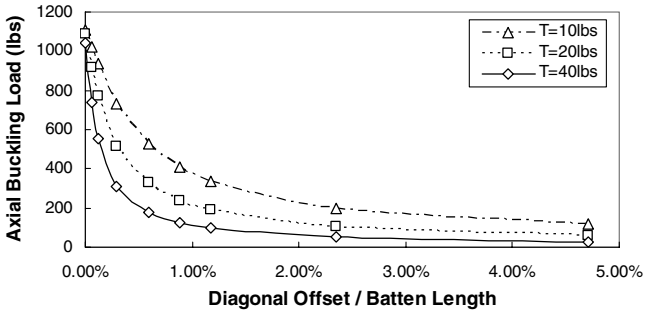

Fig. 12 Buckling load vs percent ratio of diagonal offset-to-batten length.

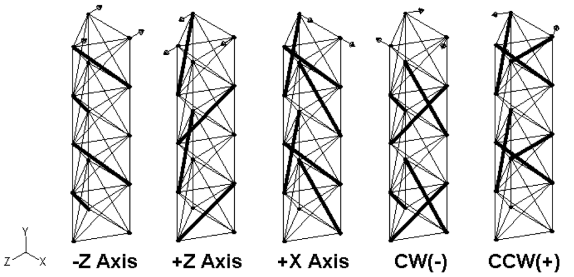

Fig. 14 Bending and torsional load directions. Stiff diagonals that slacken are highlighted.

truss (Fig. 12), they display a rapid and dramatic drop in the buckling strength, suggesting that the buckling load decreases significantly with small increases in offset and applied preload. As the offset approaches zero, the buckling load approaches that of the individual longerons, i.e., local member buckling occurs. This is expected for a truss with no offsets and the current geometry. Increasing the preload in the diagonals will 1) reduce the buckling strength of the compressed members and 2) increase the bending moment at the joints, which is also dependent on the size of the offset. However, the magnitude of both is relatively small and does not reduce the axial stiffness and critical load to the levels indicated by these buckling analyses.

Nonlinear static analyses, run at the critical values found in the buckling analyses, result in induced batten and longeron loads well below their calculated local buckling loads. The loads also do not appear to intensify significantly with increasing joint size. This counters what is seen in a FEM buckling analysis and confirms that the results in Fig. 12 represent nonphysical buckling modes. Local member buckling is identified in a static nonlinear analysis by the issuance of negative eigenvalue warnings under a given load. If the buckling mode is purely global then a sudden loss of stiffness can be observed along with large deformations and stress redistribution but warnings may not appear. As this truss structure is only four bays, and thus very stout, global buckling modes are absent.

Even though buckling in the classic sense does not occur in this structure, critical points at which there is an abrupt redistribution of stresses can be observed. A final series of static tests is run for the same preload and offset cases to find the actual loads at which a critical point is reached (Fig. 13). This is achieved by varying the axial load on the truss until negative eigenvalue warnings appear, signifying a local instability. Initially the critical load drops slightly, between offset ratios of 0.0006 and 0.06%, but then plateaus and actually increases slightly as the offset is increased from 0.06 to 1.2%. Over 1.2%, the critical load starts to diminish noticeably. The plateau and rise of the critical load for a small set of offset values is surprising, but the behavior approaches a smooth curve with increasing preload. This suggests that with low preloading, local instabilities are characterized by the nonlinear response to the joint offsets. As preload is increased, however, the base structure becomes more stable and behaves in a more conventional manner, although offset ratios below approximately 1.2% have only a minor effect on the local critical load of the truss for all preload levels. It must be noted that for a truss with a large number of bays the global buckling load would become dominant. The losses in global axial stiffness due to increased bending deformation of the vertical members can significantly reduce this load. Therefore, although the local critical loads decrease relatively slowly, one must be aware that the global buckling load of a long slender pretensioned structure could be reduced rapidly as was seen in Sec. II.D. This global behavior could be modeled by a traditional FEM buckling analysis, assuming the global modes were known to be lower than the local modes.

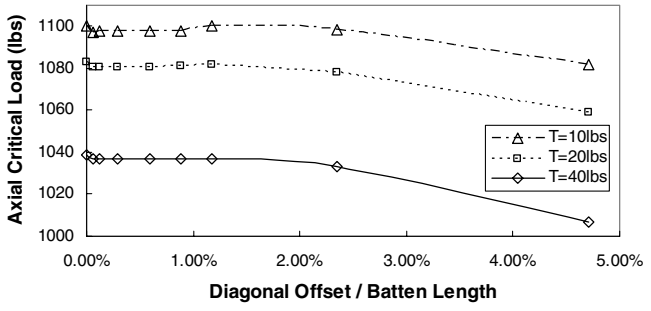

Fig. 13 Critical load vs percent ratio of diagonal offset-to-batten length.

B. Cable Slackening Under Bending and Torsion Loading

Pretensioned structures must be designed to prevent the tension members from slackening and losing stiffness. To find the point of tension loss, static load analyses must be run in bending and torsion, which impart the greatest compressive stresses on the cables. In the literature, slackened tension members are often removed from the model, which can be both tricky and time consuming. However, using the methodology of Sec. III.B, a series of static analyses are performed, using single pretensioned truss elements with the "no compression" option, that require no changes in the model during the analyses.

Bending and torsion tests are performed with a set joint size (1.2% offset) and the truss pretensioned to 10, 20, or 40 lb. The load is applied equally at the top three joints and initially aligned with the $-z$ axis. Analysis runs in the $+z$ and $+x$ directions are also performed at only a 20 lb preload to observe any differences in the point of tension loss or residual truss stiffness. The torsion analyses are run in both clockwise (CW) and counterclockwise (CCW) directions and are also compared. Figure 14 illustrates the bending and torsional cases and highlights the stiff diagonals that enter compression from the applied load. Nonlinear geometry is used as large strains are expected, and the displacements at the top nodes in the direction of load application are averaged and plotted against the total applied load. The bending or torsional stiffness of the truss, before and after tension loss, is obtained by finding the slopes of the plotted load-deflection curve.

The $-$z-axis bending analyses are plotted in Fig. 15. For all preloads, the initial and final slopes remain the same, and thus the stiffness of the truss has the same initial and final values. However, the pretension level dictates the point at which slackening occurs and

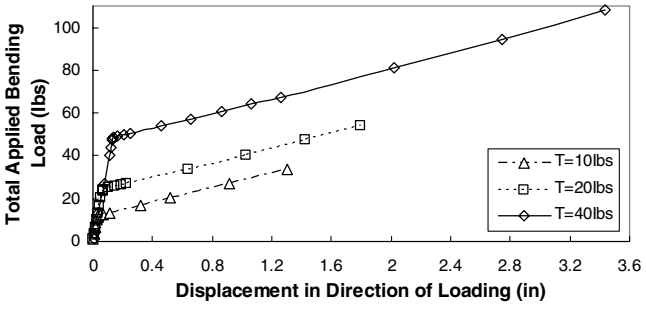

Fig. 15 Bending load in the $-$z axis vs displacement of truss.

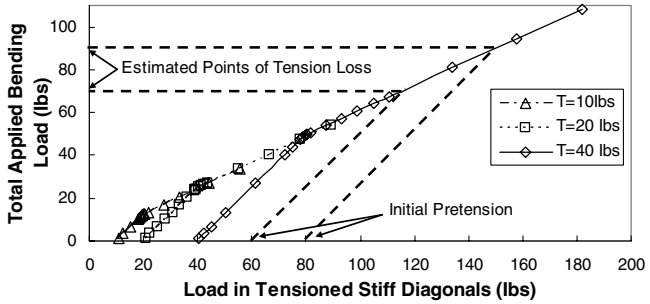

Fig. 16 Bending load in the −z axis vs tensioned stiff diagonals. Estimating tension loss.

truss stiffness drops. At that critical point, the applied load has not only provided enough compressive force to negate the preload in some members but has also overcome the additional resistance of the base structure of longerons and battens. Small load increments are used around the critical point to determine both the exact load at which the tension is lost and in which members. The stiff diagonals, highlighted in Fig. 14, slacken due to the small amount of axial deformation necessary to put them into compression. The soft diagonals are orders of magnitude less stiff and would thus require very large displacements to lose tension (effectively approximating a constant-force spring). In all bending cases, a pair of stiff diagonals loses tension at the critical point, immediately followed by the rest of those highlighted in Fig. 14. This demonstrates that, once instability is initiated by the loss of tension in one pair of members, the system must find a new equilibrium load distribution at a significantly lower global stiffness. The majority of the structural stiffness after tension loss is then provided by those stiff diagonals that are put under increasing tension, due to the direction of the applied load.

If the load in the stiff diagonals that remain tensioned is plotted against the applied load (Fig. 16), it becomes clear that the truss behavior, postslackening, is governed by these members. The initial points on the curve represent the pretension in the stiff diagonals. The load increases by the same rate in each case but is bound by the uniform bending in the truss until tension is lost. After the critical point, the tensioned stiff diagonals become the primary load bearing members, and as their elastic behavior is the same for any preload, the functions form a single line.

This plot is very useful for design purposes as it allows one to estimate the point of tension loss for a given load direction and initial preload. This is demonstrated by the dashed lines in Fig. 16. An analyst need run only one set of analyses to find the two slopes. Subsequently, a line parallel to the initial slope is drawn intersecting the x axis at the desired preload and touching the curve of the second slope. The load opposite that point on the y axis represents the approximate point of tension loss. This technique can be used with any pretensioned structure by identifying the tensioned members that go into compression first (typically the stiffest) and plotting the applied load vs the load in those members, as demonstrated.

The load vs displacement graphs for the +z- and +x-axis bending analyses yield the same initial stiffness as the −z-axis case but diverge after the point of tension loss (Fig. 17). The stiff diagonals lose tension at the same bending load for the +z-axis analysis but go into compression slightly earlier if the load is applied in the +x axis. This is due to the load being applied directly in plane with two of the stiff diagonals causing a higher local compression than for the ±Z-axis analyses. The +z case is believed to be slightly less stiff than the −z case, after tension loss, due to having only a single set of longerons at the front acting as the secondary load bearing members. In the −z case, secondary stresses are absorbed by the two sets of longerons at the back. The +x case results in the most compliant structure after tension loss, due to the location and number of slackened members. The ±z cases lose four stiff diagonals at the critical point whereas the +x case loses six. Because of the locations of the slack diagonals in the +x case, the truss also experiences more torsion than both other cases. Two diagonals slacken in two of the bays, which leads to significantly reduced torsional stiffness.

In the +x case, although two cables slacken initially as before, the remaining four do not lose stiffness immediately. It might thus be expected that, as each cable slackens, the overall structural stiffness would decrease in a stepwise manner with multiple slopes. This does not happen, however, as long as the load is applied in a constant direction, as the majority of the load is transferred from the longerons to the remaining tensioned stiff diagonals as soon as the first tension members enter compression. The stiffness lost from additional diagonals losing tension has little impact at that point as the stresses have already been redistributed. The results of these analyses illustrate that equivalent beam assumptions, often used in design of these structures, are only valid if the diagonals remain in tension. Therefore, *these assumptions must be used very carefully as tension loss can occur under much lower bending and torsional loads than would be calculated for the critical loads of an equivalent beam.*

The torsion load analyses are performed in a similar manner to the bending tests but with the loads applied tangentially at the top three points. In these analyses, all six stiff diagonals, highlighted in Fig. 14, slacken simultaneously at the critical point. As there is an even number of bays, the load distribution is equal and opposite in the two cases; thus, the point at which the cables slacken is identical. If an odd number of bays is used, the magnitude of the deflection after tension loss will be different in the CW and CCW directions due to the location of the stiff diagonals, although the critical load points will remain the same. The load-displacement plots reveal only minor differences between the CW and CCW cases (Fig. 18), with the latter producing slightly reduced residual stiffness. This is caused by small differences in the joint displacements at the top, due to the slackened top bay in the CCW case. Overall, however, the differences are minimal, as is expected.

Typically the torsional stiffness of a truss is much lower than its bending stiffness, but when tension diagonals are used, this is not necessarily true. Both the +x-axis bending analysis and the torsional analyses have the exact same point of tension loss. This occurs because the same two stiff members go into compression first (the members in common between the +x and CW cases). For more complicated asymmetric pretensioned geometries it is plausible that, as the load is increased, more than two equilibrium points could be reached. The structure, however, would have to lose tension in more than one set of stiff members. For instance, if additional support members are tensioned to higher preloads and are also compressed

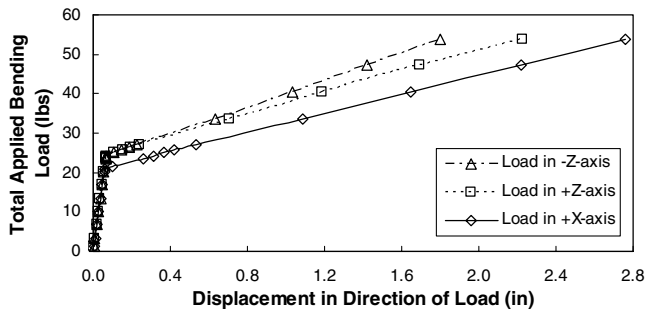

Fig. 17 Bending load vs displacement for three load directions: ±z- and +x-axes.

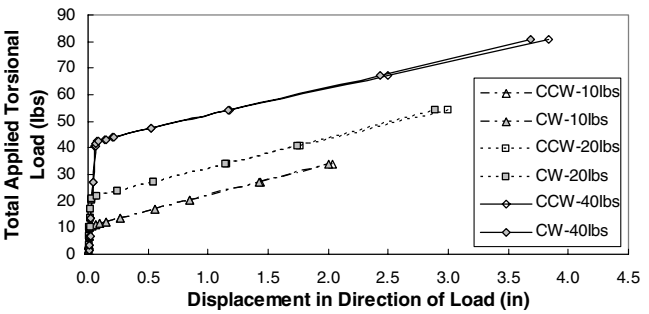

Fig. 18 Load vs displacement for a truss under torsional loads and varying pretension.

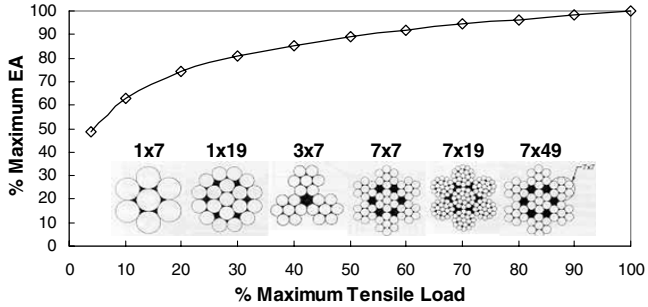

Fig. 19 Nonlinear axial stiffness of 7 × 19 steel cable vs load.

by the external loads, the structure could reach a point where these members also lose tension and the structural stiffness would be further reduced. It is thus vitally important, if static or dynamic loads are being applied to a pretensioned structure, to characterize this slackening behavior as the residual structural stiffness after tension loss is typically only 2 to 5% of the original stiffness. Tables 1 and 2 list the percent of residual truss stiffnesses and tension loss loads of the bending and torsion analyses.

C. Nonlinear Cable Stiffness Effects

Nonlinear material stiffness can occur in stays or cables that use twisted strands or fibers, such as steel cable. As the load is applied, there is some untwisting of the fibers that leads to nonlinearity at low loads. This behavior is described by a log function that relates the axial stiffness, *EA*, to the load (Fig. 19). There can be as much as a 50% drop in the cable modulus as the load approaches zero, but the effects are negligible until extremely low loads. For soft diagonals, this behavior is never a problem as the tension always remains well above zero and close to the initial preload. Conversely, the stiff diagonals that lose tension are affected, but as their stiffness is so high initially, even a 50% loss will not cause a significant change in the structural behavior of the truss. As this behavior is governed by a log function, that loss happens very close to zero load and thus the load-displacement graphs are indistinguishable from those without nonlinear stiffness cables added, i.e., there is no gradual change from the initial to final slopes.

VI. Conclusions and Modeling Recommendations

The principles and methodology for modeling and analyzing large pretensioned space structures from both a theoretical and practical perspective have been detailed. The tensioning and equilibration of these structures have been correlated to their frequency and buckling behavior, and the effects of nonlinear stiffness and geometric and load eccentricities were characterized. The key FEM issues of accurate cable and joint modeling and pretensioning the system were discussed and the methodology applied to two example structures: a simple pretensioned cable–beam system and a tensioned truss. The recommendations and approaches presented herein are derived from practical experience gained from modeling and analyzing these and other pretensioned structures.

Table 1 Percent of residual truss stiffness after tension loss

		Preload		
Load type	Load axis	10 lb	20 lb	40 lb
Bending	−z	4.87%	4.91%	5.09%
	+z	——	3.91%	——
	+x	——	5.54%	——
Torsion	CCW	3.63%	3.54%	1.93%
	CW	3.79%	3.78%	2.16%

Table 2 Applied load at point of tension loss

		Preload		
Load type	Load axis	10 lb	20 lb	40 lb
Bending	−z	12.1	24.3	48.6
	+z	——	24.3	——
	+x	——	21.6	——
Torsion	CCW	10.8	21.6	42.5
	CW	10.8	21.6	42.5

The analyst must consider several design issues while assembling a FEM model of a pretensioned structure. The local and global buckling limits of the structure must be determined and the pretension levels monitored to make sure failure does not occur. These buckling loads are affected not only by the tension but also by eccentricities in loading or geometry and the location and properties of the stays. The results of buckling, frequency, and dynamic analyses are all strongly influenced by the mass and tension in the system. Static analyses conversely are primarily dependent on the stiffness ratio and geometric arrangement of the members. The static and dynamic stiffness of the structure follows these trends, but the analyst should check for and incorporate any nonlinearities in lateral, geometric, or material stiffness into the model. Design formulas used to estimate loading on these structures should be used with caution as equivalent representations of sparse pretensioned structures will not include the severe loss of structural stiffness from cable slackening at loads significantly lower than the calculated critical loads. The limits and applicability of the chosen analysis type must also be well understood. FEM buckling analyses, for example, require an initially stiff structure and can be used only to find the global modes of pretensioned structures with eccentrically deformed members when the critical global buckling load is lower than the local buckling loads. Nonlinear static load analyses can be used to find points of local instability in these cases.

Pretensioned structures tend to be elementally sparse; thus, datum-point wire-frame modeling, in conjunction with connectors and MPCs, provides a computationally efficient way of constructing a complete structural model that can include precise joint geometry and behavior. For crossover cables, as in the truss, one must be careful to define each cable separately so that they are not considered fixed at that point. Wire-frame elements also lend themselves well to automated model construction and analysis, due to simple meshing and nodal definition. Cables can be successfully modeled using single truss elements that allow for slackening under load by using the "no compression" option in ABAQUS. This approach, used in the load analyses of the truss was shown to work very effectively for static loading. For dynamic or linear perturbation analyses, multiple beam elements can be used to model cables so long as they maintain tension such that $T \gg P_{cr}$. For structures with large numbers of tension members, using hybrid truss and beam elements avoids typical convergence difficulties associated with standard elements that do not compute bending stresses separately.

The application of pretension to a FEM model must be performed prudently and the results checked for accuracy and validity. It is recommended that pretension is applied directly by using command line input, where available (the *INITIAL CONDITIONS, TYPE = STRESS option, in ABAQUS). Alternatively, thermal strains with the selection of appropriate CTEs can be employed to similar effect. The approach used should be validated with a simple model before incorporation into a more complex structure. Pretensioning low stiffness cables yields initial and final tension levels that are approximately equal. This allows the desired final tension to be simply entered and is required for the pretension to equilibrate uniformly in structures like the tensioned truss. Higher stiffness cables, however, used in some pretensioned structures require the analyst to iterate the initial prestress until the final tension level is achieved.

This study was primarily focused on modeling methodology and only static and linear perturbation analyses were performed. However, the results of the analyses are informative. Plotting frequency vs load (Fig. 10) for a pretensioned structure allows one to determine the mass influence of the tension members, the effect of high-stiffness elements, if used, and the global buckling limit of the

system. In Sec. V, it was shown that plotting applied load vs load in the stiff residually tensioned members (Fig. 16) provides the estimated point of tension loss for any preload (below the buckling limit of the member). Future research could investigate the modeling of dynamic cable elements in a pretensioned structure in which slackening behavior interacts with and affects the modal response of the system. Modeling the dynamic deployment of these structures would be an application of this.

Acknowledgments

This study was carried out at NASA Langley Research Center, Hampton, VA, in association with the National Institute of Aerospace (NIA) and Defense Advanced Research Projects Agency (DARPA). T.C.J. and H.B.S. gratefully acknowledge the support of the National Institute of Aerospace through the Rising Star Fellowship Program.

References

[1] Mauch, H. R., and Felton, L. P., "Optimum Design of Columns Supported by Tension Ties," *Journal of the Structural Division*, Vol. 93, No. ST3, June 1967, pp. 201–209.

[2] Hofmeister, L. D., and Felton, L. P., "Prestressing in Structural Synthesis," *AIAA Journal*, Vol. 8, No. 2, Feb. 1970, pp. 363–364.

[3] Housner, J. M., and Belvin, W. K., "On the Analytical Modeling of the Nonlinear Vibrations of Pretensioned Space Structures," *Computers and Structures*, Vol. 16, No. 1–4, 1983, pp. 339–352.

[4] Miura, K., and Miyazaki, Y., "Concept of the Tension Truss Antenna," *AIAA Journal*, Vol. 28, No. 6, 1990, pp. 1098–1104.

[5] Matunaga, S., Miura, K., and Natori, M., "A Construction Concept of Large Space Structures Using Intelligent/Adaptive Structures," *Proceedings of the 31st AIAA/ASME/ASCE/AHS/ASC Structures, Structural Dynamics and Materials Conference*, Technical Papers. Part 4, AIAA, Washington, D.C., 1990, pp. 2298–2305; also AIAA Paper 1990-1128, 1990.

[6] Jasper, W. J., "Control of Large Space Structures," *AIAA 22nd Aerospace Sciences Meeting*, AIAA Paper 84-0081, Jan. 1984.

[7] Nurre, G. S., Ryan, R. S., Scofield, H. N., and Sims, J. L., "Dynamics and Control of Large Space Structures," *Journal of Guidance, Control, and Dynamics*, Vol. 7, No. 5, 1984, pp. 514–526.

[8] Hedgepeth, J. M., "Critical Requirements for the Design of Large Space Structures," NASA CR-3484, 1981.

[9] Pellegrino, S., and You, Z., "Cable-Stiffened Pantographic Deployable Structures, Part 1: Triangular Mast," *AIAA Journal*, Vol. 34, No. 4, April 1996, pp. 813-820.

[10] Belvin, W. K., "Analytical and Experimental Vibration and Buckling Characteristics of a Pretensioned Stayed Column," *Journal of Spacecraft and Rockets*, Vol. 21, No. 5, 1984, pp. 456–462.

[11] Belvin, W. K., "Vibration Characteristics of Hexagonal Radial Rib and Hoop Platforms," *Journal of Spacecraft and Rockets*, Vol. 22, No. 4, 1985, pp. 450–456.

[12] Crawley, E. F., Barlow, M. S., Van Shoor, M. C., and Masters, B., "Measurement of the Modal Parameters of a Space Structure in Zero Gravity," *Journal of Guidance, Control, and Dynamics*, Vol. 18, No. 3, May–June 1995, pp. 385–394.

[13] Easley, S., Adler, A., Dichter, B., Ginet, G., Granata, J., Hausgen, P., Spanjers, G., Winter, J., Cohen, D., Davis, L., and Kemper, S., "The AFRL DSX Flight Experiment," *Space 2004 Conference and Exhibit*, AIAA Paper 2004-5892, Sept. 2004.

[14] Fang, H., and Lou, M. C., "Analytical Characterization of Space Inflatable Structures—An Overview," *40th AIAA/ASME/ASCE/AHS/ASC Structures, Structural Dynamics, and Materials Conference and Exhibit*, AIAA Paper 1999-1272, April 1999.

[15] Pai, P. F., and Young, L. G., "Modeling, Analysis and Testing of Some Deployable/Inflatable Structures," *45th AIAA/ASME/ASCE/AHS/ASC Structures, Structural Dynamics, and Materials Conference and Exhibit*, AIAA Paper 2004-1797, April 2004.

[16] Taleghani, B. K., Sleight, D. W., Muheim, D. M., Belvin, K. W., and Wang, J. T., "Assessment of Analysis Approaches for Solar Sail Structural Response," *39th AIAA/ASME/SAE/ASEE Joint Propulsion Conference and Exhibit*, AIAA Paper 2003-4796, July 2003.

[17] Thornton, E. A., Dechaumphai, P., and Pandey, A. K., "Finite Element Thermal-Structural Analysis of a Cable-Stiffened Orbiting Antenna," *26th Structures, Structural Dynamics, and Materials Conference and Exhibit*, AIAA Paper 1985-693, April 1985, pp. 308–315.

[18] Thornton, E. A., and Paul, D. B., "Thermal-Structural Analysis of Large Space Structures: An Assessment of Recent Advances," *Journal of Spacecraft and Rockets*, Vol. 22, No. 4, July–Aug. 1985, pp. 385–393.

[19] Wada, B. K., Kuo, C. P., and Glaser, R. J., "Multiple Boundary Condition Tests (MBCT) for Verification of Large Space Structures," AIAA Paper 86-0905, May 1986.

[20] *ABAQUS Example Problems Manual*, ABAQUS Standard/CAE Software Package, Ver. 6.4, ABAQUS, Inc., Providence, RI, 2003, Secs. 1–9.

[21] Mukhopadhyay, M., *Vibrations, Dynamics and Structural Systems*, 2nd ed., A. A. Balkema Publishers, Rotterdam, The Netherlands, 2000.

[22] Timoshenko, S. P., and Gere, J. M., *Theory of Elastic Stability*, 2nd ed., McGraw–Hill, New York, 1961.

[23] Blevins, R. D., *Formulas for Natural Frequency and Mode Shape*, Litton Educational Publishing, Inc., New York, 1979.

L. Peterson
Associate Editor